The Japan Society of Mechanical Engineers

Study on the Thermal Shock Behavior of Cermets and Cemented Carbides*

Sotomi ISHIHARA**, Takahito GOSHIMA**, Kazyu MIYAO**, Takashi YOSHIMOTO*** and Shinichi TAKEHANA**

Thermal shock behavior of cermets and cemented carbides was studied in detail by using unnotched smooth bar specimens. Thermal shock was applied to the specimens by plunging them into a water bath at 290 K. After thermal shock experiments, bending strength, micro-Vickers hardness and fracture toughness of the specimens were investigated. As a result, two different types of thermal shock behavior were observed between cermets and cemented carbides. This difference indicates that microcracks occur more easily in cemented carbides than in cermets during thermal shock experiments.

Key Words: Thermal Shock, Bending Strength, Vickers Hardness, Fracture Toughness, Microcrack, Cermets, Cemented Carbides

1. Introduction

It is well known that many thermal cracks are initiated during cutting work, such as high-speed cutting and intermittent cutting[1]. In order to develop a good cutting tool, it is necessary to study the thermal shock behavior of the tool material. Concerning the thermal shock behavior of ceramics, many studies have been performed[2]~[5], but there have been few studies on cermets and cemented carbides[6].

In this study, thermal shock behavior for both cermets and cemented carbides was studied by investigating the variations of bending strength, micro-Vickers hardness and fracture toughness due to thermal shock tests. As a result, it was clarified that the thermal shock behaviors of cermets and cemented carbides differ from each other.

* Received 24th May, 1991. Paper No. 90-0151A
** Faculty of Engineering, Toyama University, 3190 Gofuku, Toyama 930, Japan
*** Fujikoshi Corporation, Ishigane, Toyama 930, Japan

2. Specimens and Experimental Procedures

2.1 Specimens

The materials used in this test were cermets and cemented carbides, and their chemical compositions are listed in Table 1(a) and Table 1(b), respectively. Microstructures for the materials are shown in Fig. 1. Specimens were made by pressing the particle into the shape shown in Fig. 2. The mechanical properties of the materials are listed in Table 2.

2.2 Experimental procedures

Thermal shock was applied to the specimens by heating them in a furnace for 30 minutes and then plunging them into a water bath at 290 K. The temperature difference ΔT_w between the furnace and the water bath was employed as a scale for the severity of thermal shock. After thermal shock tests, three-point bending tests were performed to investigate the relation between the residual strength of the specimen after thermal shock and ΔT_w. The span of the bending test was 20 mm and the crosshead speed was 0.01 mm/min.

The specimens' hardness was measured by using the micro-Vickers hardness tester. The fracture

NII-Electronic Library Service

The Japan Society of Mechanical Engineers

Table 1 Chemical compositions of the materials

(a) Cermets wt%

TiCN	TaC	WC	Ni	Co	Mo
50	10	15	8	8	9

(b) Cemented carbides wt%

WC	TiC	TaC	NbC	Co
72	8	8	2	10

Table 2 Mechanical properties of the materials

	Young's modulus GPa	Poisson's modulus
Cermets	428.26	0.233
Cemented carbides	527.24	0.222

toughness of each specimen was also measured by the Vickers indentation method using the expression proposed by Miyoshi et al[7]. Ten to twenty measurements were made after the thermal shock test.

3. Experimental Results

3.1 Bending strength of specimens subjected to thermal shock

Figure 3 shows the experimental relationship between the bending strength of the specimens after thermal shock and the temperature differences which exhibit the severity of the thermal shock. As seen from this figure, the bending strength of cermets is nearly constant between $\Delta T_w = OK$ and 495 K, but in the region above 495 K, it falls steeply and becomes 10% of the initial value. Therefore, the critical temperature difference ΔT_{wc} for cermets is found to be 495 K. On the other hand, the critical temperature difference of cemented carbides is 1.24 times larger than that of cermets. But the bending strength of cemented carbides decreases gradually with an increase of ΔT_w even under the critical temperature difference, showing a different behavior from that of

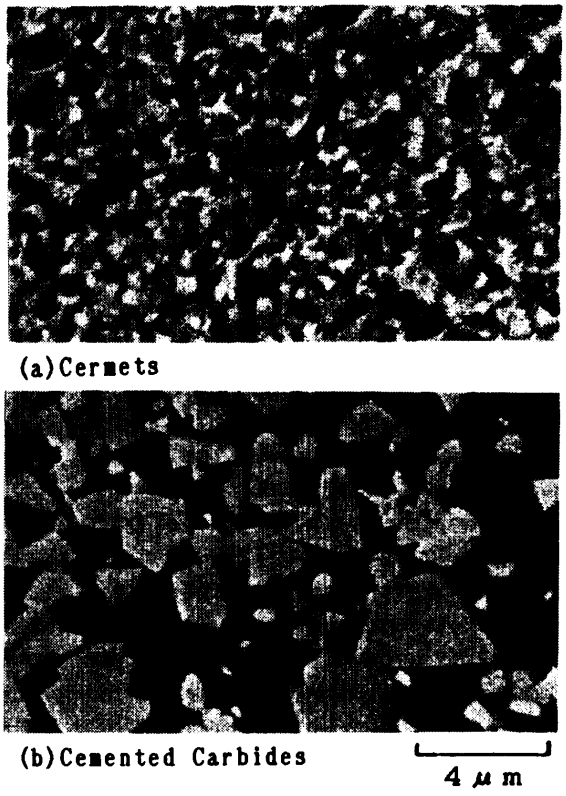

Fig. 1 Microstructures of the materials

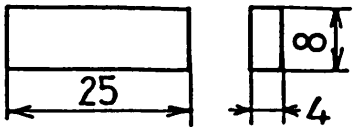

Fig. 2 Shape and dimensions of the specimen

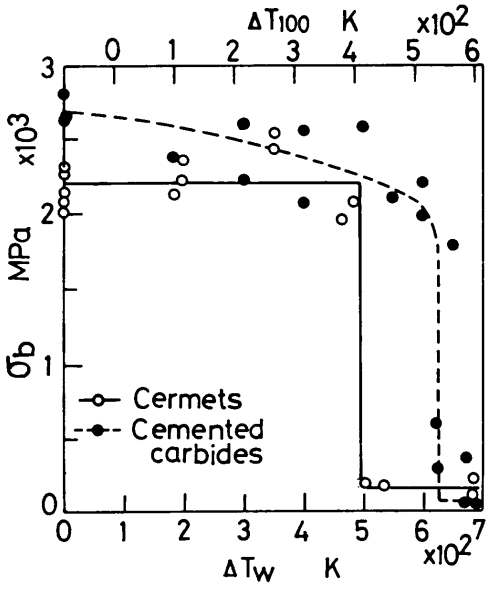

Fig. 3 Variations of bending strength due to thermal shock

NII-Electronic Library Service

The Japan Society of Mechanical Engineers

cermets.

3.2 The variation of each specimen's hardness after thermal shock

Figure 4 shows the relationships between micro-Vickers hardness of each specimen after thermal shock and the temperature difference. The solid and broken lines in this figure represent the average value of the hardness. In cermets, the hardness increases monotonously from 14 000 MPa to 15 200 MPa with an increase in the temperature difference. In cemented carbides, on the other hand, the hardness is unchanged with an increase in the temperature difference, showing a nature different from that of cermets.

3.3 Fracture toughness of the specimen subjected to thermal shock

Figure 5 shows the variation of fracture toughness due to thermal shock. The solid and broken lines in this figure represent the mean value of fracture toughness. As seen from the results of the cermets, the values of fracture toughness decrease with an increase in the temperature difference. However, in cemented carbides, the values of the fracture toughness are nearly constant until $\Delta T_w = 300$ K, where they decrease with increasing temperature difference.

4. Considerations

4.1 Estimation of the Biot modulus in the thermal shock test

Figure 6 shows large cracks which appeared on the smooth specimen surface subjected to the thermal shock in which the temperature difference is above the critical temperature difference. Therefore, at the thermal shock of the critical temperature difference, it is considered that the stress intensity factor of the maximum crack reaches the fracture toughness of the material tested, causing the ultimate fracture of the specimen. The discussion below is based on the experimental result mentioned above.

The stress intensity factor for the surface cracks (crack length: $2a$, crack depth: b) to which the tensile stress σ is applied, is represented by the following equation[8]

$$K_I = \sigma Y_1 (\pi b)^{1/2}, \quad (1)$$

where Y_1, is the correction factor. The thermal stress σ induced by the change in the temperature is given by the next equation,

$$\sigma = \alpha E \Delta Tw / \{(1-\nu) f(\beta)\}, \quad (2)$$

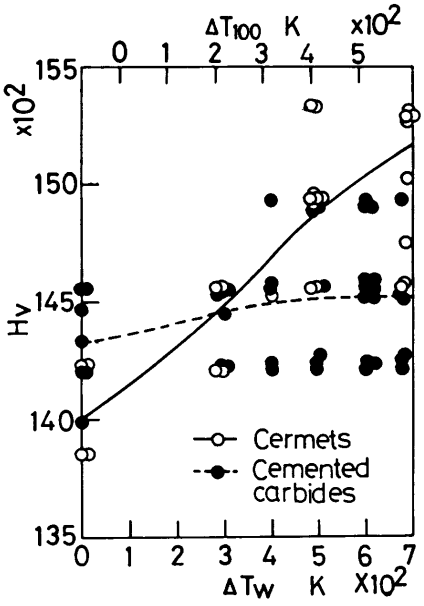

Fig. 4 Variations of micro-Vickers hardness through thermal shock

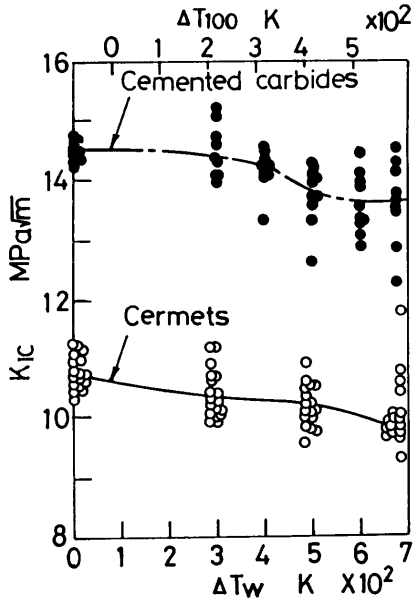

Fig. 5 Variations of fracture toughness through thermal shock

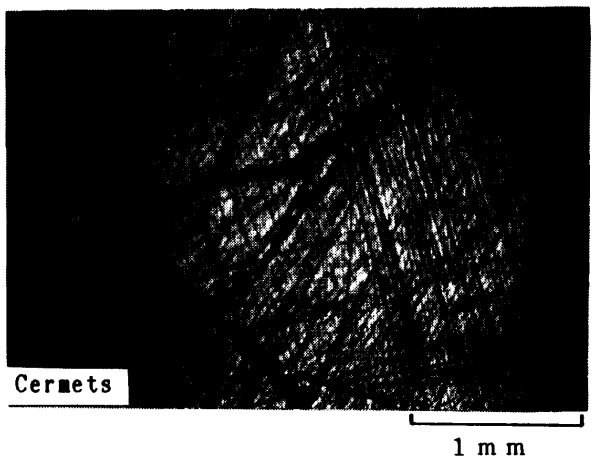

Fig. 6 Appearance of large cracks due to thermal shock in the region above critical temperature difference

NII-Electronic Library Service

The Japan Society of Mechanical Engineers

where α is the coefficient of thermal expansion, E is Young's modulus, ν is Poisson's modulus, β is the Biot modulus and $f(\beta)$ is the function of the Biot modulus. Substituting Eq.(2) into Eq.(1) and using the condition $K_I=K_{IC}$ at $\Delta T_w=\Delta T_{wc}$, we obtain the following equation:

$$K_{IC}=\alpha E\Delta T_{wc}Y_I(\pi b)^{1/2}/\{(1-\nu)f(\beta)\}, \quad (3)$$

where $f(\beta)$ is expressed as

$$f(\beta)=1.5+B/\beta-0.5\exp(-16/\beta) \quad (B=3.25). \quad (4)$$

Neglecting the temperature dependence of the material constants such as K_{IC}, α, and E, we obtain the linear relation between ΔT_{wc} and b whose slope is -0.5 on the log-log plot from Eq.(3).

Single thermal shock tests were performed on the precracked specimens. Precracks were introduced by the micro-Vickers hardness tester. The crack aspect ratio b/a was 0.74. The temperature difference ΔT_w at which the precracks started to grow to about 10 μm was investigated for the specimens having various precrack lengths $2a$. Figure 7 shows the relationship between precrack length $2a$ and the temperature difference ΔT_w. If we regard these temperature differences ΔT_w as the critical temperature differences ΔT_{wc}, then Fig. 7 is considered to be an experimental illustration of Eq.(3). As seen from Fig. 7, the linear relationships are observed on the log-log plot, and their slopes are -0.5 for both cermets and cemented carbides. The same phenomenon as found in this investigation was also observed for ceramics by Akiyama et al.[3].

Three-point bending tests were also conducted using precracked specimens. Figure 8 shows the relationship between bending strength σ_b and precrack length $2a$ on the log-log plot. From this figure, we can evaluate fracture toughness for both materials using the expression of Raju and Newmann[8].

As a first approximation, let us consider the fact that the values of fracture toughness obtained from the above method are nearly equal to those in the present thermal shock tests. Then, we can evaluate the Biot modulus of the present test by using both Eq. (3) and Fig. 7. The estimated values of the Biot modulus are 316 and 54 for cermets and cemented carbides, respectively. These values are large enough to indicate the severe thermal shock conditions for both materials. In the evaluation of the Biot modulus, the coefficients of thermal expansion, 7.96×10^{-6} and 5.34×10^{-6} are used for cermets and cemented carbides, respectively. These values are not measured, but calculated using the law of mixture. Furthermore, the temperature dependence of the material constants was not considered.

From the above discussion, for cermets, thermal stress induced by thermal shock can be approximated by

$$\sigma=\alpha E\Delta T_w/(1-\nu). \quad (5)$$

For cemented carbides, thermal stress is considered to be nearly 84% of Eq.(5).

4.2 Estimation of the amount of crack growth due to thermal shock

Ashizuka et al[5], who studied the thermal shock behavior of zirconia, considered both the effect of crack growth and the phase transformation of the material during thermal shock as main factors influencing the thermal shock phenomenon in the region below the critical temperature difference. In the materials used, the effect of the phase transformation is considered to be small in the present temperature region; thus, only crack growth which occurs during thermal shock will be discussed.

The critical temperature difference ΔT_{wc} is found from Eq.(3) as

$$\Delta T_{wc}=K_{IC}(1-\nu)f(\beta)/\{\alpha EY_I(\pi b)^{1/2}\}. \quad (6)$$

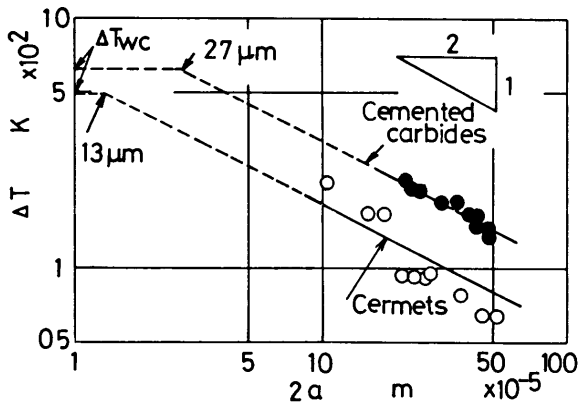

Fig. 7 Relationship between crack length $2a$ and ΔT at which the precrack starts to grow to about 10 μm

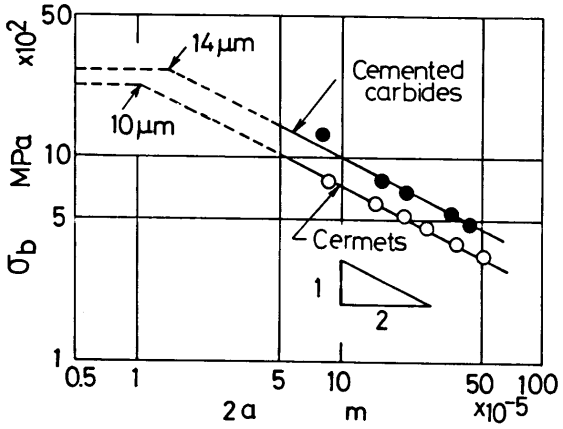

Fig. 8 Relationship between bending strength σ_b for the precracked specimens and precrack length $2a$

NII-Electronic Library Service

The Japan Society of Mechanical Engineers

This expression shows that ΔT_{wc} is in proportion to K_{IC} and is in inverse proportion to a, E and $b^{1/2}$. If we suppose that no cracks can initiate and grow during the thermal shock test, the latent crack lengths in the specimens before the thermal shock test can be estimated from Fig. 8 as 10 μm and 14 μm for cermets and cemented carbides, respectively. Using these values, we can calculate ΔT_{wc} as 541 K and 877 K from Eq. (6) for cermets and cemented carbides, respectively. Comparing these estimated values with the experimental values, we find that both values are nearly equal for cermets, while for cemented carbides, the estimated value is considerably larger than the experimental value. The error in this estimation is considered to be due to the neglect of any crack growth which occurred during the thermal shock tests.

The fracture toughness does not change through a single thermal shock until ΔT_w=400 K. Considering this experimental fact, we can evaluate the amount of crack growth due to thermal shock using both the relation σ_b-ΔT_w shown in Fig. 3 and the relation σ_b-$2a$ shown in Fig. 8. Figure 9 shows the estimated amount of crack growth. The solid and broken lines correspond to cermets and cemented carbides, respectively. The solid marks in this figure represent the crack lengths at the critical temperature differences estimated from the ΔT_w-$2a$ relation of Fig. 7. These marks correspond well to the solid and broken lines, so we can confirm the validity of this estimating method. As seen from Fig. 9, in cemented carbides, a crack grows from 14 μm to 25 μm through a thermal shock of ΔT_w=OK to 613 K. Recalculating the critical temperature difference for cemented carbides, as $2a$=25 μm in Eq.(6), we obtain the result of ΔT_{wc}= 675 K. This value is nearly the same as the experimental value of 613 K. On the other hand, in cermets, a crack does not develop through a thermal shock until ΔT_w=495 K. The result corresponds well to the phenomenon that no decrease in bending strength was observed until ΔT_w=495 K in the σ_b-ΔT_w relation of Fig. 3.

For cemented carbides, it was concluded that the crack growth which occurred during thermal shock in the region below the critical temperature difference caused the decrease in the bending strength of the specimen.

4.3 The difference between cermets and cemented carbides in the variation of hardness and fracture toughness due to thermal shock

By taking into account both the strain-hardening and the crack growth through a thermal shock, we can explain the variations in hardness and fracture toughness between cermets and cemented carbides. That is, both materials are strain-hardened through a thermal shock, but in cemented carbides, small cracks are apt to initiate and grow due to thermal shock, and these cracks cause relaxation of the strain-hardening and prevent the decrease in fracture toughness. In cermets, on the other hand, small cracks are hard to initiate, and no relaxation of the strain-hardening occurs.

4.4 Effect of microstructure of the materials on crack initiation and growth behavior in thermal shock

We can consider cermets and cemented carbides as hybrid materials which are composed of a ductile binder phase and a hardened brittle phase. As seen from the micrograph of Fig. 1, the hardened brittle phases are TiCN and WC for cermets and cemented carbides, respectively, and the ductile binder phases are Ni and Co for cermets and Co for cemented carbides. Figure 10 shows the simple model for the microstructure of the materials in which the binder phase and the hardened phase are restricted at their extremes in only the y direction. The restriction in the x direction is neglected for simplicity. In this case,

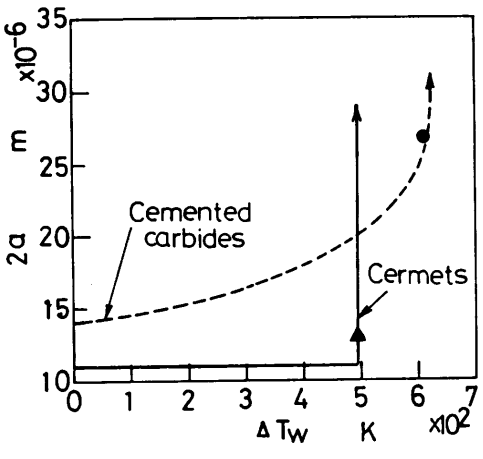

Fig. 9 Estimated crack growth curves during the thermal shock tests

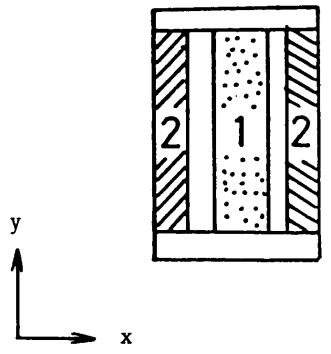

Fig. 10 A model of the material microstructures

NII-Electronic Library Service

The Japan Society of Mechanical Engineers

thermal stresses σ_1 and σ_2 in the phases due to the change of the tempersture ΔT are given by

$$\sigma_1=-(\alpha_1-\alpha_2)\Delta T A_2E_1E_2/(A_1E_1+A_2E_2)$$
$$\sigma_2=(\alpha_1-\alpha_2)\Delta T A_1E_1E_2/(A_1E_1+A_2E_2), \quad (7)$$

where α, E and A are the coefficient of thermal expansion, Young's modulus and the cross area, respectively.

To simplify the problem, letting $\Delta T=A_1=A_2=1$, we obtain the following expressions:

$$\sigma_1=-(\alpha_1-\alpha_2)E_1E_2/(E_1+E_2)$$
$$\sigma_2=(\alpha_1-\alpha_2)E_1E_2/(E_1+E_2). \quad (8)$$

From the above expressions, we realize that the larger the values of $(\alpha_1-\alpha_2)$ and E become, the larger the thermal stresses become.

In cemented carbides, the coefficients of thermal expansion for the hardened phase (WC) and the binder (Co) are $3.84\times10^{-6}\,K^{-1}$ and $12.3\times10^{-6}\,K^{-1}$ respectively. In cemented carbides, because the difference in the coefficient of thermal expansion between the two is considerably large and the value of Young's modulus is also large (696 GPa), thermal stresses become fairly large and cause microcracks at the interface between WC and Co. On the other hand, in cermets, the coefficients of thermal expansion for the hardened phase (TiCN) and the binder (Ni, Co) are $9.35\times10^{-6}\,K^{-1}$ and $13.3\times10^{-6}\,K^{-1}$ respectively. As both the difference between these values and the Young's modulus (215~451 GPa) are not large, it is considered that thermal stresses are not sufficient to initiate thermal cracks in cermets.

5. Conclusions

Thermal shock tests were performed on cermets and cemented carbides, and the results obtained are summarized as follows:

(1) The critical temperature differences ΔT_{wc} are 495 K and 613 K for cermets and cemented carbides, respectively. In cemented carbides, due to thermal shock below the critical temperature difference, bending strength decreased with an increase in the temperature difference. In cermets, the bending strength was nearly constant in the region below the critical temperature.

(2) Different behavior was observed between cermets and cemented carbides in the relations H_V-ΔT_w and K_{IC}-ΔT_w. In cermets, increased hardness and decreased fracture toughness were observed with an increase of ΔT_w. In cemented carbides, there was no change with an increase of ΔT_w.

(3) Two factors, that is, crack initiations and hardening due to a thermal strain, correspond to the different thermal shock behavior between cermets and cemented carbides. In cermets, crack initiations through thermal shock occur less often than they do in cemented carbides, so no decrease in the bending strength due to crack initiations in the region below the critical temperature difference was observed, and hardening due to thermal strain caused a decrease in the fracture toughness. In cemented carbides, crack initiations readily occur, so bending strength decreased even in the region below the critical temperature difference, but the hardness and fracture toughnesses were not changed by thermal shock because hardening due to thermal strains is relaxed by crack initiation.

(4) By considering cermets and cemented carbides as composite materials which are composed of a brittle hardened phase and a ductile binder phase, and by modeling them, we can explain the difference between cermets and cemented carbides by the crack initiation and growth behavior which occurs during thermal shock.

(5) In order to estimate the critical temperature difference ΔT_{wc} in the thermal shock tests, crack growth which occurs during thermal shock must be considered in addition to the material constants such as fracture toughness K_{IC}, the coefficients of thermal expansion and Young's modulus E.

References

(1) Iyori, Y., Sima, N. and Ida, H., Development of High-Toughness Cermet, Technological Report of Hitachi Kinzoku, (in Japanese), Vol. 5(1987), p. 65.

(2) Maekawa, I., Shibata, H., Kobayashi, A. and Wada, T., Thermal Shock Fatigue of Al_2O_3 Ceramics, J. Soc. Mater. Sci. Jpn., (in Japanese), Vol. 38, No. 429(1989), p. 658.

(3) Akiyama, S., Kimura, Y. and Sekiya, M., Evaluation of Thermal Shock Resistance in Cersmic Materials, J. Soc. Mater. Sci. Jpn., (in Japanese), Vol. 38, No. 435(1989), p. 1415.

(4) Kamiya, N. and Kamigaito, O., Thermal Fatigue Life of Ceramics under Mechanical Load, J. Mater. Sci., Vol. 17, No. 11 (1982), p. 3149.

(5) Ashizuka, M., Kimura, Y., Fujii, H., Abe, K. and Kubota, Y., Thermal Shock Behavior of Y_2O_3-Partially Stabilized Zirconia, Yougyou Kyoukai, (in Japanese), Vol. 94, No. 6 (1986), p. 577.

(6) Suzuki, K., Fujiwara, T. and Usui, S., Effect of WC Grain Size on Oxidation and Thermal Shock-Resistance of WC-20% Co Sintered Alloys, J. Jpn. Inst. Metals, (in Japanese), Vol. 40, No. 3(1976), p. 211.

(7) Miyoshi, T., Sagawa, N. and Sassa, T., Evaluation of Fracture Toughness in Ceramics, Trans. Jpn. Soc. Mech. Eng., (in Japanese), Vol.51, No.471, A (1985), p. 2489.

(8) Raju, I. S. and Newmann, J. C., Eng. Fract. Mech., Vol. 11(1979), p. 817.

NII-Electronic Library Service